Carbon-carbon bond formation and hydrogen production in the ketonization of aldehydes

Lina M. Orozco,[a] Michael Renz*[a] and Avelino Corma*[a]

Abstract: Aldehydes possess a relatively high chemical energy which is the driving force for disproportionation reactions such as Cannizzaro or Tishchenko reaction. Generally, this energy is wasted when aldehydes are transformed into carboxylic acids with a sacrificial oxidant. Here, we describe a cascade reaction in which the surplus energy of the transformation is liberated as molecular hydrogen when heptanal is oxidized to heptanoic acid by water and the carboxylic acid is transformed into potentially industrially relevant symmetrical ketones by ketonic decarboxylation. The cascade reaction is catalyzed by *monoclinic* zirconium oxide (*m*-ZrO_2). The reaction mechanism has been studied by performing cross coupling experiments between different aldehydes and acids, and it is shown that the final symmetrical ketones are formed by a reaction pathway that involves the previously formed carboxylic acids. Isotopic studies indicate that the carboxylic acid can be formed by a hydride shift from the adsorbed aldehyde to the metal oxide surface in absence of noble metals.

Introduction

Carbon–carbon bond formation reactions are important transformations for processing biomass derived molecules to produce chemicals and fuels.[1-4] Biomass-based platform molecules derived from pentose and hexoses possess in most cases five or six carbon atoms while fuel molecules are typically in the range from C_9 to C_{15} for kerosene and from C_9 to C_{20} for diesel fuel. Therefore, reactions that involve carbon–carbon bond formation will be required to produce kerosene[6, 7] and diesel[8, 9] starting from cellulose and hemicellulose. One strategy for the above, involves the deoxygenation and decarboxylation to yield C_4–C_6 olefins[7, 10] that are then oligomerized. However, it is possible to take advantage of the reactivity introduced by oxygen functionalities to form carbon-carbon bonds selectively. Hence, other routes involve aldol condensation reactions[6, 11, 12] of aldehydes and ketones and the ketonic decarboxylation[13-15] (also called ketonization)[2] of carboxylic acids.

In the two last routes it is the carbonyl group which introduces certain reactivity into the molecule. Carbonyl compounds are CH-acidic in α-position and the carbonyl carbon can act as an electrophilic center. This reactivity has been demonstrated to be the origin of the two reactions named above, i.e. aldol condensation and ketonization. The mechanism of the aldol condensation (Scheme 1) is widely accepted and starts with the deprotonation of an aldehyde or a ketone forming an anion which then attacks a second molecule (aldehyde or ketone). Water elimination provides the α,β-unsaturated carbonyl compound. On the other hand, the mechanism of the ketonization of carboxylic acids was under debate until recently.[15] The combination of experimental studies and density functional theory calculations has revealed that this reaction starts with a double deprotonation of one acid molecule (Scheme 2). A second molecule is dehydroxylated and the electrophilicity at the carbonyl carbon is increased. Hence, in a similar way as for the aldol condensation, the negatively charged α-carbon atom attacks the carbonyl carbon. The formed intermediate is then decarboxylated to provide the ketone (Scheme 2).

The intrinsic reactivity of the molecules and catalytic procedures which have been developed make both reactions valuable tools for synthetic organic chemistry, providing predictable products with high selectivity. A related reaction that has received much less attention is the transformation of two molecules of aldehyde into a ketone. Formally it can be considered as an oxidation of the aldehyde to the corresponding carboxylic acid (Eq. 1) with subsequent ketonic decarboxylation of the latter (as described above; Scheme 2).[16] However, the mechanism is still under debate: disproportionation of Cannizzaro or Tishchenko-type may provide the acid (derivative) for subsequent ketonic decarboxylation.[17-20] Alternatively, aldol condensation products are discussed as intermediates, which are then dehydrogenated and decarboxylated.[16, 21-25] Furthermore, this reaction is not restricted to aldehydes as starting materials, but primary alcohols can also be converted to symmetrical ketones.[22, 26-28]. In this case, the aldehyde is supposed to be produced *in*-situ and converted to the ketone.

Manifold materials have been employed in the transformation of aldehydes and alcohols during decades: CeO_2, Y/CeO_2, Pd/CeO_2, Co/CeO_2, CeO_2–MgO_2, CeO_2–Fe_2O_3, ZrO_2, $Ce_xZr_{1-x}O_2$, Cr/ZrO_2, Pd/m-ZrO_2, ZnO_2, MgO, ThO_2, La_2O_3, $Cu/La_2Zr_2O_7$, Fe_3O_4, Fe_2O_3–ZnO, Sn–Ce–Rh oxide.[16, 17, 20-22, 24, 25, 27-35] Many of them involve a redox-active element such as iron, cerium or chromium, or a noble metal, for instance for alcohol dehydrogenation. In some cases, consumption of surface

[a] Mrs. L. M. Orozco, Dr. M. Renz, Prof. Dr. A. Corma
Instituto de Tecnología Química,
Universitat Politècnica de Valencia-Consejo Superior de Investigaciones Científicas (UPV - CSIC),
Av. de los Naranjos s/n, E-46022 Valencia, Spain.
E-mail: acorma@itq.upv.es, mrenz@itq.upv.es

Supporting information for this article is given via a link at the end of the document.

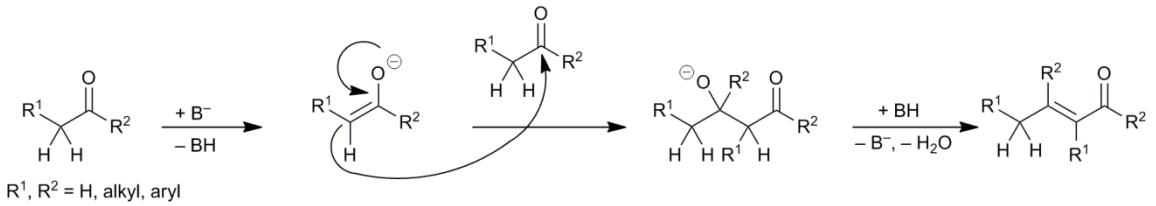

Scheme 1. Reaction mechanism of the aldol condensation.

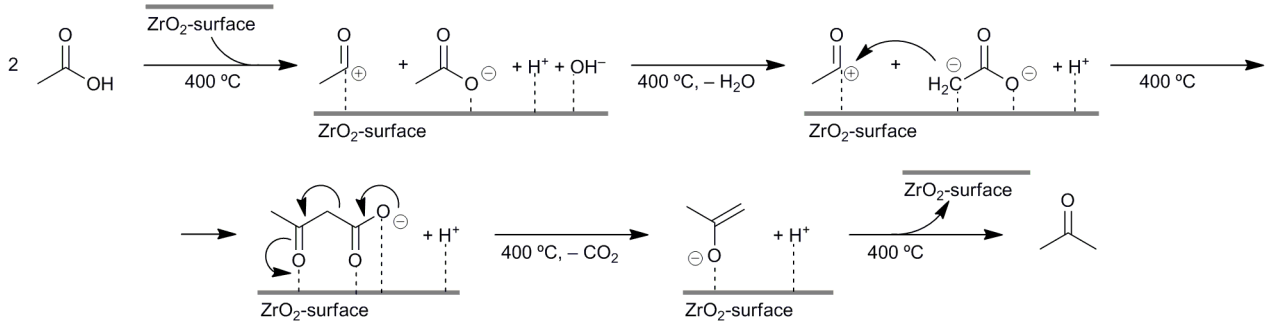

Scheme 2. Reaction mechanism for the ketonic decarboxylation on a ZrO_2 surface as described in [5]

oxygen atoms for aldehyde oxidation is discussed as in the case of CeO_2.[24, 31, 33] It seems that the redox-functionality is a requirement for smooth reaction, although redox inactive metal oxides have also been reported as catalysts.[19] Zirconium oxide has been reported as a catalyst for ketonization of aldehydes[19, 20, 36] but it has also been claimed to favor aldol condensation over ketonization of aldehydes.[37]

Herein, we use *monoclinic* zirconium oxide, *m*-ZrO_2, as a bifunctional and non-reducible catalyst for the transformation of aldehydes into ketones. Hence, heptanal has been converted into 7-tridecanone with a selectivity of up to 66% and molecular hydrogen is observed as a reaction product. It is shown that water increases the selectivity by suppressing the formation of the aldol condensation product. It is further demonstrated that water acts as a reaction partner and one proton is used to form molecular hydrogen and the hydroxy group is incorporated into the carboxylic acid. Hence, oxidation of aldehyde to carboxylic acid by water is supported in the present manuscript by means of kinetic and isotopic studies.

Results and Discussion

Catalyst characterization

Two high surface materials, *m*-ZrO_2 and *t*-ZrO_2, with *monoclinic* and *tetragonal* phase respectively (103 and 150 $m^2\ g^{-1}$, respectively, entries 1 and 3 in Table 1) and one zirconium oxide, *m*-ZrO_2-A, with a low surface area and *monoclinic* phase (4 $m^2\ g^{-1}$, entry 2 in Table 1) were used in the present work together with a cerium oxide material with redox properties and a high surface area of 114 $m^2\ g^{-1}$ (similar to *m*-ZrO_2; see Table 1). In the case of the high surface area (> 100 $m^2\ g^{-1}$) materials, the pore diameter is within a range between 40 to 90 Å, which correspond to mesopores (entries 1, 3 and 4 in Table 1). Also the mesopore volume is high, varying from 0.14 to 0.24 $cm^3\ g^{-1}$. In contrast, the metal oxide with low surface area, *m*-ZrO_2-A, has almost no porosity (entry 2).

Other Zr-containing materials such as ZrO-MCM-41 and Zr-MCM-41 were synthesized and $ZrSiO_4$ was used as a reference for the ones above (entries 5 to 7). Zr-MCM-41 was obtained by direct synthesis, adding the zirconium precursor to the synthesis gel of the structured mesoporous silicate. In contrast, ZrO-MCM-41 was prepared by impregnating a zirconium precursor ($ZrO(NO_3)_2$) onto the calcined MCM-41 material. Both materials have isolated zirconium sites coordinated to up to four silyloxy groups or di- or tri-metallic active centers where zirconium atoms are connected by oxygen bridges.[38] The grafted material has all zirconium sites on the surface whereas in the direct synthesis material zirconium should substitute silicon atoms of the wall. The mesoporous structure of the materials was confirmed by X-ray diffraction (Figure S1) and surface area was approximately 700 $m^2\ g^{-1}$ in both cases (Table 1, entries 5 and 6). The amount of zirconium incorporated was determined by ICP-OES and was found to be 1.6 wt% and 2.8 wt% for ZrO-MCM-41 and Zr-MCM-41, respectively. These isolated Zr centers possess Lewis acidity as it has been shown by *in-situ* IR spectroscopy of adsorbed cyclohexanone.[38]

The acidity of the ZrO_2 and CeO_2 materials was determined by temperature-programmed desorption of ammonia (TPD-NH_3). Figure 1 displays the corresponding profiles and it can be seen that for ZrO_2 they are very similar for all the high surface area materials (> 100 $m^2\ g^{-1}$). Ammonia desorption occurs between 250 and 300 ºC. Interestingly, dehydration was observed starting at 200 ºC with increasing intensity up to 600 ºC. The dehydration

Table 1. Physical and morphological properties of the catalysts.

Entry	Catalyst	S_{BET}[a] [$m^2\ g^{-1}$]	D_p[b] [Å]	V_p[c] [$cm^3\ g^{-1}$]	Reducible sites[d] [wt% (ºC)]	Acid sites[e] [µmol g^{-1} (wt%)]
1	*m*-ZrO_2	103	87.9	0.24	< 1	170 (2.1)
2	*m*-ZrO_2-A	4	202.7	0.00	< 1	20 (0.3)
3	*t*- ZrO_2	150	39.3	0.14	1	180 (2.2)
4	CeO_2	114	47.2	0.15	9.8 (462) 12.2 (727)	20 (0.4)
5	ZrO-MCM-41	670	26.2	0.17		
6	Zr-MCM-41	737	29.3	0.35		
7	$ZrSiO_4$	[f]	[f]	0.11		

[a]Specific surface area calculated by the BET method using N_2 adsorption isotherm at −196 ºC. [b]Pore size. [c]Pore volume. [d]From TPR measurements. [e]From TPD measurements. [f] Not measurable.

is more pronounced for the *monoclinic* material than for the *tetragonal* one. For the *m*-ZrO_2-A material the acidic sites were hardly detected (not shown), certainly due to the low surface area. The NH_3-TPD profile of CeO_2 shows a maximum between 300 and 450 ºC. However, the MS detector indicates that the signal is not related to ammonia desorption but predominately to dehydration. Therefore, it has to be concluded that the amount of acidic sites is equally low as for the low surface zirconium acid *m*-ZrO_2-A (Table 1, entries 2 and 4). The X-ray diffraction pattern of the oxide materials are given in Figure 2. The XRD pattern of *m*-ZrO_2 corresponds to the *monoclinic* phase. From the X-ray diffractograms, it can be concluded that *m*-ZrO_2 is *monoclinic* and *t*-ZrO_2 is purely *tetragonal*. However, a contamination of *m*-ZrO_2 with the *tetragonal* phase cannot be excluded since all the corresponding signals overlap and the broadness of the bands makes a differentiation impossible. CeO_2 exhibited a cubic phase of fluorite. High surface area materials, formed by small crystallites, give broader peaks than the sample with larger particles and low surface which exhibits sharper signals.

The TPR profile for pure CeO_2 showed two distinct regions. A low temperature region (300–600 ºC) with a maximum at around 470 ºC attributed to the surface reduction of the Ce^{4+} ions, and a high temperature region (700–900 ºC),[39] with a maximum at around 750 ºC, probably related to the reduction of the bulk oxide (Figure 3).[31] In the case of the zirconium oxide reducibility is more than one order of magnitude lower than for cerium oxide. This is well in accordance with literature where zirconium oxide is considered to be a non-reducible material.[14, 31] Especially *m*-ZrO_2 did not show any peak in the TPR profile (Figure 3) and the concentration of the reducible sites was lower than 1 wt% (Table 1, entry 1). Residual reducibility may result from remaining organic parts of the metal precursors.

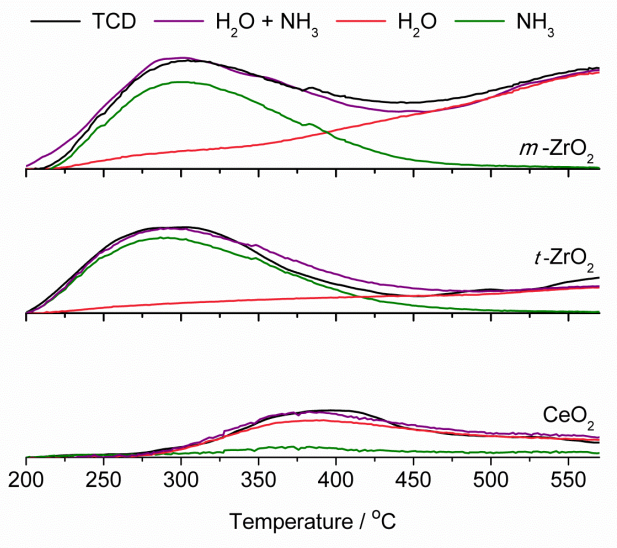

Figure 1. Profiles of the temperature-programmed desorption of ammonia (TPD-NH_3) carried out on *m*-ZrO_2, *t*-ZrO_2 and CeO_2.

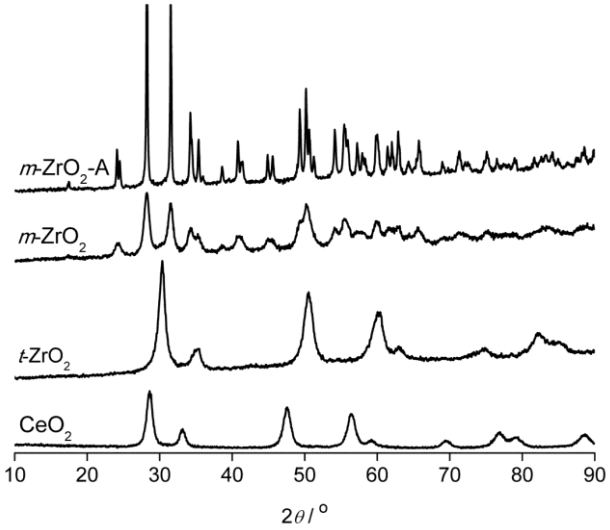

Figure 2. X-ray diffraction (XRD) pattern of *m*-ZrO_2-A, *m*-ZrO_2, *t*-ZrO_2 and CeO_2.

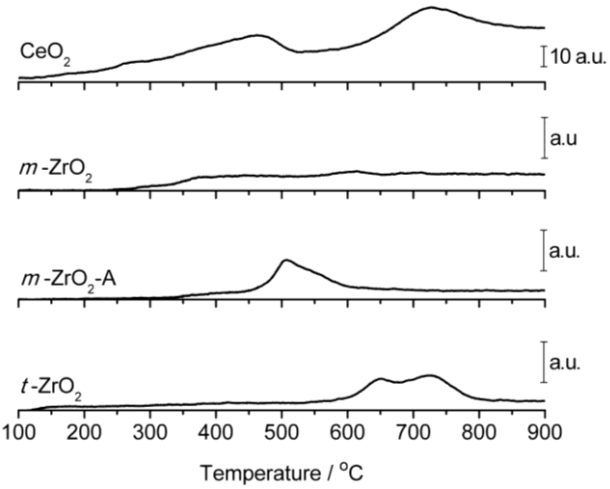

Figure 3. Profiles of the temperature-programmed reduction (TPR) of CeO_2, *m*-ZrO_2, *m*-ZrO_2-A, *t*-ZrO_2.

IR spectroscopic measurements of the thermally treated high-surface area zirconium oxides indicate that the surface is highly hydrated at room temperature (Figure 4). Heating both phases, *tetragonal* and *monoclinic*, at 300 ºC in vacuum (10^{-2} to 10^{-3} Pa) the water desorbs and two different types of surface hydroxyl groups become evident. Furthermore, it can be concluded that Lewis acidic surface sites are made accessible which were occupied by the water before its desorption. In the carbonyl region (1600 to 1400 cm^{-1}) traces of organic residues from the metal precursors can be detected.

Figure 4. Infrared (IR) spectra of self-supporting wafers of *t*-ZrO_2 and *m*-ZrO_2 outgassed at room temperature, at 300 and 400 ºC.

Ketonization of heptanal over monoclinic zirconium oxide and related materials

Heptanal was chosen as model substrate since the size of the molecule facilitates the condensation of the products when performing the reaction in a fixed bed continuous-flow reactor. Heptanal is available as biomass derived platform molecule by thermal treatment of methyl ricinoleate or castor oil.[40, 41] In the literature the ketonization of aldehydes has been reported in presence[19, 31] and absence[20, 24, 27] of water and a beneficial effect of the water on the ketone selectivity has been observed. Therefore, both conditions were assessed in our study.

Since zirconium oxide exists with two stable phases at low temperature, i.e., *monoclinic* (*m*-ZrO_2) and *tetragonal* (*t*-ZrO_2), both phases were considered in the present study. The results obtained should also be compared to cerium oxide which is a well-known catalyst for the ketonization of aldehydes.[31, 42]

Before carrying out the catalyst screening, the reaction temperature was selected by working with *m*-ZrO_2 as catalyst (Figure 5). Reaction temperature had to be raised to 400 ºC to observe a conversion of 20 to 30%, in presence or absence of water, and a further increase to 450 ºC provided almost full conversion. The corresponding ketone, i.e., 7-tridecanone, was achieved in 67% and 37% yield in presence and absence of water, respectively. Interestingly, in absence of water the aldol condensation product was observed in approx. 23% yield whereas in presence of water it was observed only in traces. From these first survey 450 ºC was selected as standard reaction temperature for studying the catalytic activity of the catalysts.

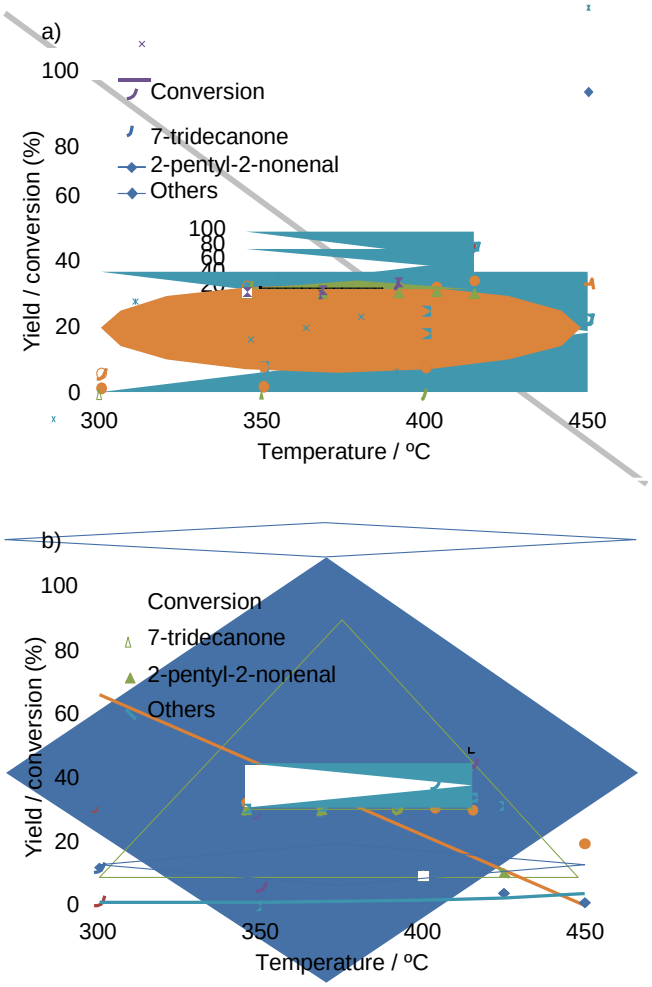

Figure 5. Conversion and product yields for the ketonization of heptanal over *m*-ZrO_2 in the absence (a) and presence (b) of water as a function of reaction temperature. Reaction conditions: heptanal-water molar ratio 1 : 8 (5 mL of heptanal, 0.2 mL min^{-1}), 0.204 mL min^{-1} water, 50 mL min^{-1} N_2 and 1 g of catalyst.

The catalytic results stated before were achieved with a zirconium oxide material (*m*-ZrO_2) with high surface area (103 m^2 g^{-1}, Table 1, entry 1) and *monoclinic* structure. When a material with the same crystalline phase but with a very low surface area (< 5 m^2 g^{-1}, cf. Table 1, entry 2) was employed, i.e. *m*-ZrO_2-A, conversion dropped to 15% without co-feeding water and below 10% when adding water to the feed (Table 2, entry 2). When the initial reaction rates were normalized by catalyst surface areas, the values obtained were much closer indicating that the active sites were the same and the surface area was the main fact that explains activity differences.

When zirconium sites were incorporated in silica MCM-41 either by a postsynthesis (ZrO-MCM-41) or by a direct synthesis procedure (Zr-MCM-41), the ketonization reaction did not take place (Table 2, entries 3 and 4). Aldehyde conversion is rather low, and the main products were condensation products. This result indicates that various neighbored sites with well-defined geometrical arrangement on the zirconium oxide surface should be involved in the ketonization. On the other hand, when the crystallographic phase of zirconium oxide was changed from *monoclinic* to *tetragonal*, while maintaining a high surface area (150 m^2 g^{-1}, Table 1, entry 3), the conversion remained complete under our reaction conditions (Table 2, entry 5), but the yield of the desired ketone, 7-tridecanone, dropped from 37% (entry 1) to 5% (entry 5), without co-feeding water and from 67% to 16% in presence of water. Probably, the origin of the different catalytic activity is the different coordination sphere of the zirconium centers in the monoclinic and the tetragonal phase: in the first case the metal atom is surrounded by seven oxygen atoms and in the second case by eight.[43] In any case, from this comparison it can be seen that not only several sites are involved in the ketonization but also the geometrical arrangement is important. It can then be stated that the crystalline phase is decisive for the catalytic activity of zirconium oxide and that the *monoclinic* phase is the most active one.

Comparison with a zirconium silicate indicate again that the reactions observed are not due to the simple presence of zirconium sites nor to thermal transformations. The conversion obtained with this material was as low as 6% (Table 2, entry 6). No ketone was observed and only traces of the condensation products were detected.

The results obtained with *monoclinic* zirconium oxide (*m*-ZrO_2) were also compared with CeO_2, which is a classical catalyst for the ketonization of aldehydes as it was mentioned before. When the reaction was carried out co-feeding water the yield for the ketone was practically the same on the two catalysts (Table 2, entry 1 and 7). However, without co-feeding water the yield with CeO_2 was 54% versus 37% with *m*-ZrO_2. This comparison demonstrated that *m*-ZrO_2 is a suitable catalyst for the ketonization of aldehydes and that the catalytic performance when co-feeding water is at the same level than the best catalyst reported up to now. The fact that, contrary to *m*-ZrO_2, the reaction catalyzed by CeO_2 is less influenced by water, will be explained later.

Reaction stoichiometry

The gaseous products, i.e. hydrogen and carbon dioxide produced during the ketonization reaction were monitored and quantified. Two equivalents of hydrogen and one equivalent of carbon dioxide were obtained per equivalent of ketone, regardless of co-feeding water or not (Table 2, entries 1 and 7), with *m*-ZrO_2 and CeO_2.

For *m*-ZrO_2, the reaction was run for a prolonged time on stream until the production of almost 100 g of substrate per gram of catalyst (Figure 6). With this amount of substrate passed, steady state was achieved. Therefore, under these conditions, the amount of zirconium oxide can be considered as a stabilized catalyst that does not intervene in the stoichiometry.

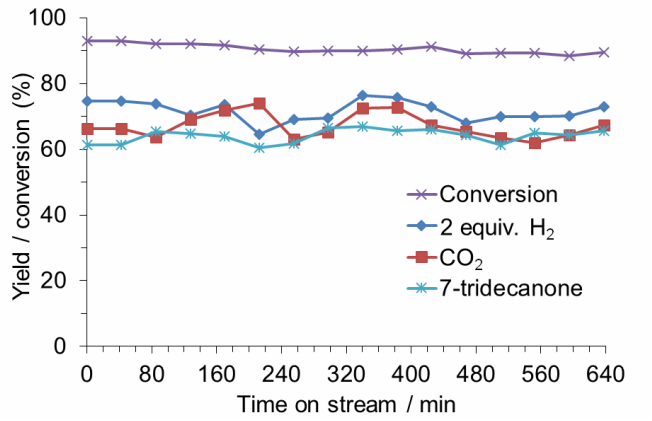

Figure 6. Catalytic performance of *m*-ZrO_2 with time on stream in the ketonization of heptanal. Yield calculated per 2 equiv. of aldehyde; stoichiometry can be consulted in Eq. 2. Reaction conditions: heptanal-water molar ratio 1 : 8, 0.2 mL min^{-1} heptanal, 0.204 mL min^{-1} water, 50 mL min^{-1} N_2 and 450 ºC. During the reaction 110 g of heptanal were passed per g of catalyst.

Furthermore, results from Figure 6 indicate that the catalytic activity is stable with time on stream. During this time on stream the yield of the three main products, i.e. 7-tridecanone, hydrogen and carbon dioxide, remained constant and the stoichiometry correspond to two molecules of aldehyde that are converted into one molecule of ketone, one molecule of carbon dioxide and two molecules of hydrogen (Eq. 2).

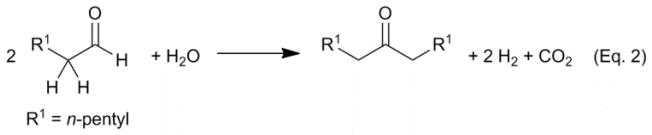

The atomic balance of Eq. 2 can be achieved by adding one water molecule as substrate. Then, if water is required as reactant for the process to occur, the question is how the reaction can proceed in absence of water. Results from Table 2 indicate that water is formed during reactions such as, for instance, aldol condensations. This means that even in the case that water is not added to the feed, some water will always be present during the reaction. Therefore, there are two issues that require further investigation, such as the role of water in the reaction, and the formation of two moles of H_2 per mol of ketone formed.

Role of water on product selectivity

It was reported above that water improves the selectivity towards the ketone product while water is consumed for the formation of ketone. Taking that into account, one could expect that water would enhance the reaction rate for the formation of the ketone. To check this hypothesis kinetic measurements were carried out in the absence of water and in the presence of

Table 2. Heptanal conversion and principal product yields over different catalysts for the ketonization of heptanal. Reaction conditions: 1.0 g of catalyst was placed in a fixed bed and heptanal (5 mL, 0.2 mL min^{-1}) was reacted in the gas phase in a continuous-flow reactor at 450 ºC under nitrogen flow (50 mL min^{-1}), feeding heptanal-water molar ratio 1 to 8 (0.204 mL min^{-1} water). Numbers in parentheses indicate conversion and yield without co-feeding water.

			Yield[a]							
Entry	Catalyst	Conv. [%]	C_{13}-Ketone [%]	Aldol Cond. Prod.[b] [%]	Aldol Cond. Isomer.[c] [%]	Ketone Fragments[d] [%]	Others[e] [%]	2 H_2[f] [%]	CO_2 [%]	CO [%]
1	*m*-ZrO_2	90 (95)	67 (37)	1 (23)	5 (15)	13 (4)	5 (16)	69 (42)	65 (33)	2 (5)
2	*m*-ZrO_2-A	8 (15)	1 (1)	1 (1)	2 (3)	0 (1)	4 (9)	2 (2)	4 (4)	0 (1)
3	ZrO-MCM-41	68 (58)	2 (5)	1 (1)	3 (2)	8 (2)	54 (48)	0 (0)	1 (3)	4 (37)
4	Zr-MCM-41	6 (27)	1 (4)	0 (1)	1 (1)	0 (1)	4 (21)	1 (1)	2 (4)	2 (4)
5	*t*-ZrO_2	65 (99)	16 (5)	10 (2)	8 (5)	4 (14)	27 (73)	16 (16)	23 (20)	9 (5)
6	$ZrSiO_4$	(6)	(0)	(0)	(1)	(1)	(4)	(0)	(2)	(0)
7	CeO_2	87 (96)	66 (54)	1 (3)	1 (13)	12 (10)	8 (16)	68 (45)	54 (29)	3 (14)

[a] Yield calculated with respect to the aldehyde substrate taking into account the reaction stoichiometry: two aldehyde molecules form one ketone molecule or one molecule of the other products. [b] Yield for the aldol condensation product. [c] Yield for isomerized dimers with the same mass as the aldol condensation product but different retention times in GC. [d] C_8–C_{11} ketone fragmentation products; probably derived from the ketone product. [e] Other products observed in the liquid phase and quantified by GC. For more information on this group see Table S1 in Supp. Inf. [f] Yield of two equiv. of molecular hydrogen per two equiv. of aldehyde substrate.

increasing amounts of water. Surprisingly, no beneficial effect on the reaction kinetics was detected (Figure 7), but the ketone formation was fastest in the absence of water. Interestingly, a similar negative effect of water on the reaction rate was observed for the ketonic decarboxylation of carboxylic acid (Figure 8). Taking into account these results we could assume, in a first approximation, that H_2O competes with the aldehyde for adsorption to surface sites, decreasing the rate of reaction, or may retard the reaction rate at a later stage.

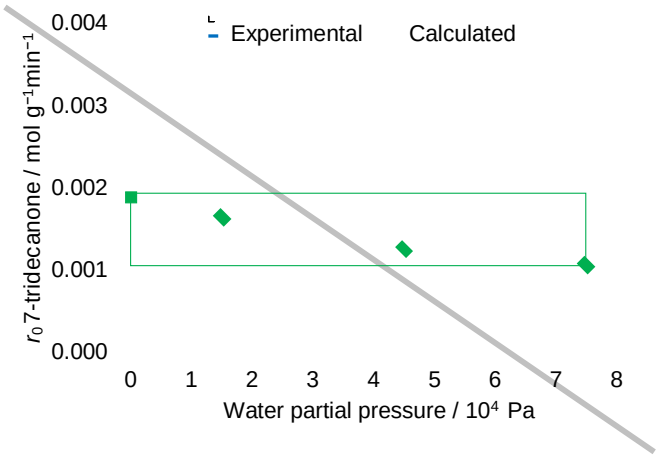

Figure 7. Initial rates for the ketonization of heptanal at partial pressure of 1.5 10^4 Pa with *m*-ZrO_2 in the presence of different amounts of water (0, 1.5, 4.5 and 7.5 10^4 Pa). Reaction conditions: heptanal (5 mL, 0.147 mL min^{-1}), heptanal : water molar ratio 1 : 1 (0.019 mL min^{-1} water, 118 mL min^{-1} N_2, 6, 15, 23 mg of catalyst), 1 : 3 (0.056 mL min^{-1} water, 67 mL min^{-1} N_2, 8, 15, 23 of mg catalyst) and 1 : 5 (0.094 mL min^{-1} water, 16 mL min^{-1} N_2, 15, 30, 50 mg of catalyst), 450 ºC; without water the reaction was carried out with 5, 16 and 22 mf of catalyst and 144 mL min^{-1} N_2. For details on the calculated line see kinetic part.

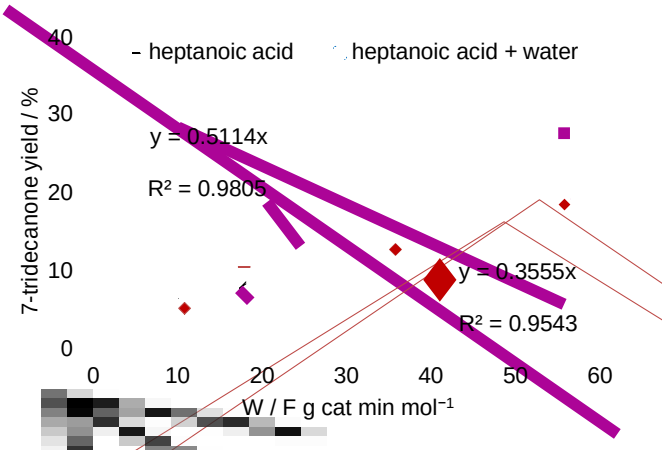

Figure 8. Yields of ketone at different contact times W/F for the ketonization of heptanoic acid at partial pressure of 10^4 Pa with *m*-ZrO_2 in absence and presence of water. Reaction conditions: heptanoic acid (5 mL, 0.041, 0.064, 0.128 and 0.213 mL min^{-1}), N_2 (71, 111, 222, 365 mL min^{-1}), heptanoic acid : water molar ratio 1 : 8, water (0.041, 0.065, 0.130, 0.216 mL min^{-1}), N_2 (15, 23, 46, 77 mL min^{-1}), 15 mg catalyst, 450 ºC.

Water also influences the rate of accompanying reactions such as the aldol condensation between two aldehyde molecules (Scheme 3). In absence of water, aldol condensation was observed as a competitive reaction pathway, which is considerably decreased in presence of water. Aldol condensation is an equilibrium reaction in which water is co-produced (Scheme 3). Therefore, the addition of water might shift the aldol equilibrium towards the substrate, i.e. the aldehyde, that can follow the desired ketonization pathway. As the ketonization reaction is irreversible, the product selectivity is shifted successively towards the ketone.

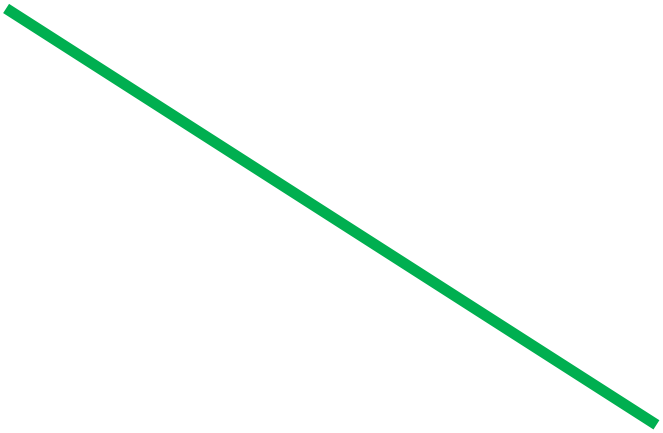

Scheme 3. Two alternative reaction pathways for heptanal: aldol condensation and ketonization. As the aldol condensation is an equilibrium reaction, the presence of additional water may shift this reaction towards the aldehyde which can then react via ketonization. Hence, water improves the yield of the ketone.

With the aim to check this hypothesis, the aldol condensation product (99% purity), together with water, was submitted to the reaction conditions. Notice that to avoid the results to be masked by the direct transformation of the aldol condensation product into the ketonization product,[6, 11, 12] the reaction was carried out in the presence of an aldehyde with different chain length, i.e. hexanal. Then, if the aldol condensation was reversible under the employed reaction conditions the cross-coupling ketonization product of hexanal and heptanal, i.e. 6-dodecanone, has to be observed. This was indeed the case, and 6.5% of 6-dodecane was observed whereas 7-tridecanone was only formed in 2.3%. Interestingly, the amounts for all three ketonization products are very similar to those obtained when a comparable mixture of hexanal and heptanal is reacted (cf. cond. II, Scheme 4): 7.8% of 6-dodecane and 2.2% of 7-tridecanone. This result clearly indicates that the role of water was the suppression of by-products by shifting the equilibrium of side reactions towards the substrate. Then, since CeO_2 gives lower amounts of aldol condensation than *m*-ZrO_2, a smaller effect of the added water can be expected in the former (cf. above). The cross-coupling experiment also proved unequivocally that the aldol condensation product was not an intermediate towards the ketonization product since if this was the case, the yield of 7-

tridecanone would have been higher than the yield of 6-dodecanone.

Mechanism of the ketonization reaction

The reaction mechanism for the ketonization of aldehydes is still under debate.[21] In our case, we presented above that the aldol condensation product can be excluded as intermediate for the formation of the ketone. Now a possible reaction pathway that involves the oxidation of the aldehyde followed by ketonic decarboxylation of the corresponding carboxylic acid derivate will be considered.

Along this line, an experimental observation was the presence of heptanoic acid in the product mixture in low yield (1–2%) when working in the presence of water (Figure 9). Furthermore, when the yield is plotted versus conversion, the shape of the curve indicates that heptanoic acid is a primary and unstable product. At conversions lower than 5% the yield of heptanoic acid is even higher than the yields of 7-tridecanone and the aldol condensation product.

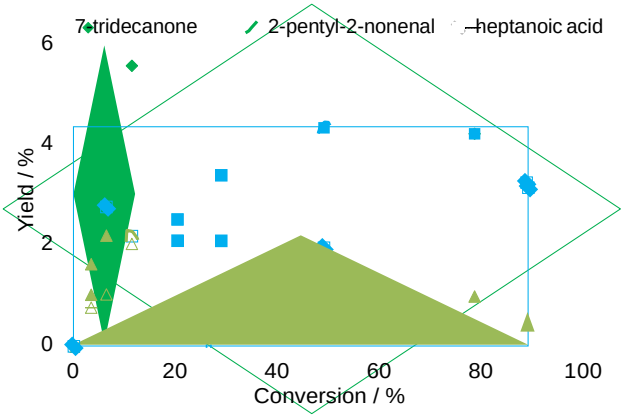

Figure 9. Yield over conversion of 7-tridecanone, 2-pentyl-2-nonenal (aldol condensation product) and heptanoic acid. Reaction condition: heptanal : water ratio 1 : 5, heptanal (5 mL, 0.147 mL min^{-1}, 10^4 Pa partial pressure), 0.094 mL min^{-1} water, 16 mL min^{-1} N_2, 0.1, 0.2, 0.4, 0.6, 0.8 and 1 g of *m*-ZrO_2, 450 ºC.

Nevertheless the fact that the carboxylic acid was detected as a primary unstable product, it is not a definitive proof for its participation in the ketonization of aldehydes. Then, with the aim to demonstrate this participation unequivocally, the cross-coupling of heptanal was carried out in the presence of the same molar amount of hexanoic acid under ketonization conditions (Scheme 5). If the ketonization of aldehydes does not proceed through the formation of the corresponding acid, one could expect the hexanoic acid to react via the ketonic decarboxylation to 6-undecanone, whereas heptanal should be converted into 7-

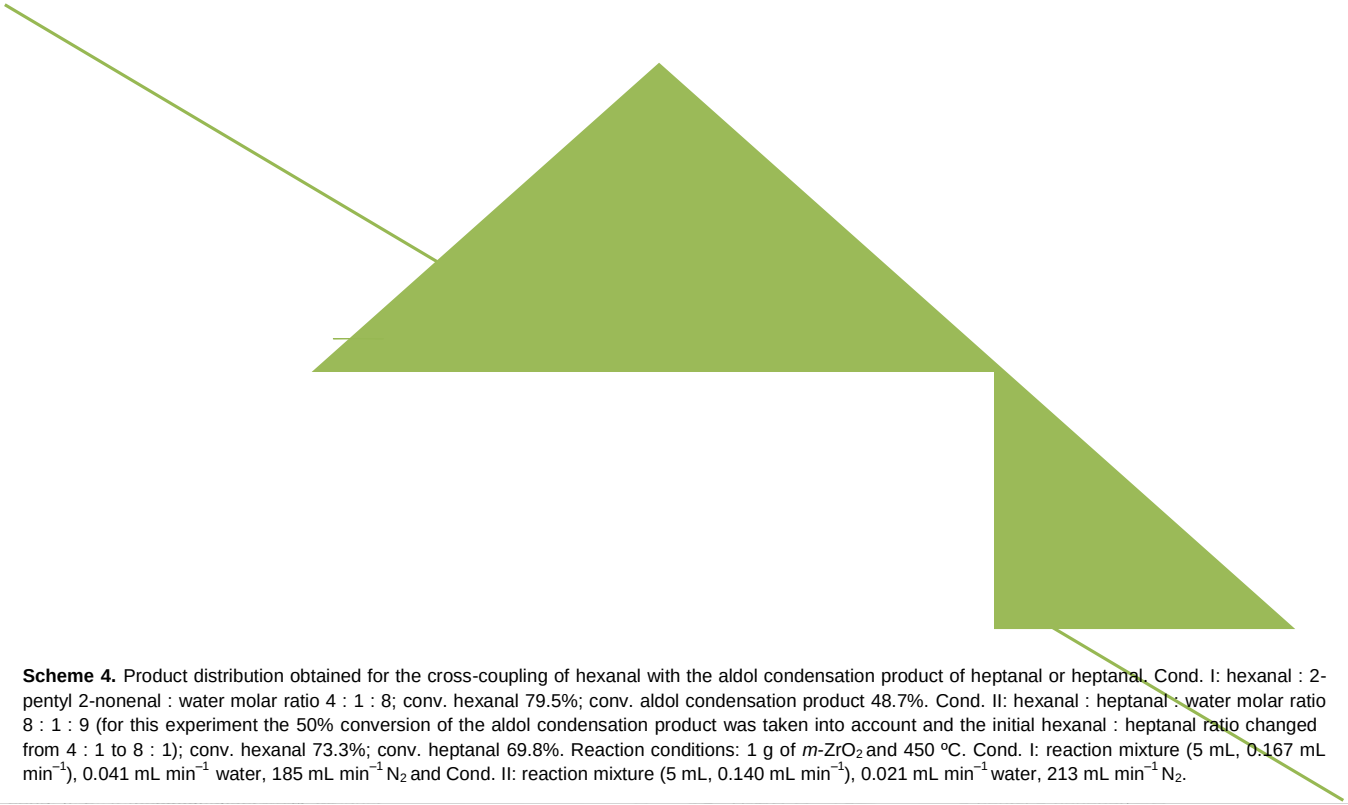

Scheme 4. Product distribution obtained for the cross-coupling of hexanal with the aldol condensation product of heptanal or heptanal. Cond. I: hexanal : 2-pentyl 2-nonenal : water molar ratio 4 : 1 : 8; conv. hexanal 79.5%; conv. aldol condensation product 48.7%. Cond. II: hexanal : heptanal : water molar ratio 8 : 1 : 9 (for this experiment the 50% conversion of the aldol condensation product was taken into account and the initial hexanal : heptanal ratio changed from 4 : 1 to 8 : 1); conv. hexanal 73.3%; conv. heptanal 69.8%. Reaction conditions: 1 g of *m*-ZrO_2 and 450 ºC. Cond. I: reaction mixture (5 mL, 0.167 mL min^{-1}), 0.041 mL min^{-1} water, 185 mL min^{-1} N_2 and Cond. II: reaction mixture (5 mL, 0.140 mL min^{-1}), 0.021 mL min^{-1} water, 213 mL min^{-1} N_2.

tridecanone as main product by aldehyde ketonization. In other words, both products will be generated by self-condensation reactions. However, if the carboxylic acid is formed as an intermediate for the ketonization reaction when starting from the aldehyde, an additional product should be observed, i.e. the cross coupling between heptanoic and hexanoic acids to give 6-dodecanone. The results obtained show the formation of 16% yield of 6-dodecanone (Scheme 5). Nevertheless, the 16% yield was lower than the yield obtained (48%) when both carboxylic acids, instead of acid and aldehyde, were reacted (Scheme 5). This result could be explained by considering that the ketonic decarboxylation is faster than the oxidation of the aldehyde to the carboxylic acid under the present reaction conditions (cf. *Kinetic study*). Hence, initial carboxylic acid is consumed rapidly and a low amount remains for the cross coupling reaction at a later stage of the reaction.

Scheme 5. Product distribution obtained for the cross-coupling of aldehyde with carboxylic acid with a different number of carbon atoms compared to the cross-coupling of two carboxylic acids with the corresponding chain lengths. Reaction conditions: reaction mixture 1: heptanal (R= –H) and hexanoic acid (R= –OH), molar ratio 1 : 1; reaction mixture 2: heptanoic acid and hexanoic acid, molar ratio 1 : 1; reaction mixtures (5 mL, 0.2 mL min^{-1}), 50 mL min^{-1} N_2, 1 g *m*-ZrO_2, 450 ºC. Water was not fed. Conversion > 99%.

In any case, the important result from the experiment was the appearance of the cross coupling product which can only be formed from the two corresponding carboxylic acids, i.e. hexanoic and heptanoic acid. Therefore, it can be concluded that heptanal is oxidized to heptanoic acid under the ketonization conditions and the carboxylic acid is a reaction intermediate.

The formation of the carboxylic acid intermediate is also in accordance with the empirical reaction equation obtained from the long term experiment (Eq. 2). Hence, two aldehyde molecules are oxidized with two molecules of water giving carboxylic acid and molecular hydrogen (Eq. 3). In the next step, the two molecules of carboxylic acid can react via the classical ketonic decarboxylation reaction to produce the ketone, carbon dioxide and water (Eq. 4). When combing both reactions, Eq. 5 is obtained which corresponds exactly with the molecular stoichiometry found experimentally.

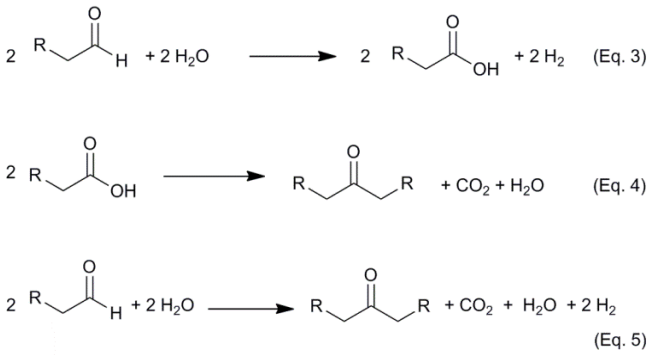

It is remarkable that water acts as terminal oxidant and hydrogen is produced. It is clear that the driving force for this oxidation is not the oxidation power of water but the high enthalpy of formation of the aldehydes.[44] The latter is also the driving force for the disproportionation reactions of aldehydes, i.e. the Cannizzaro and the Tishchenko reactions. Water is a mild oxidant and it is not active at low temperatures (below steam reforming temperatures). However, thermodynamic calculations have shown that the transformation depicted in Scheme 6 (balanced equation) is favorable for propanal.[24]

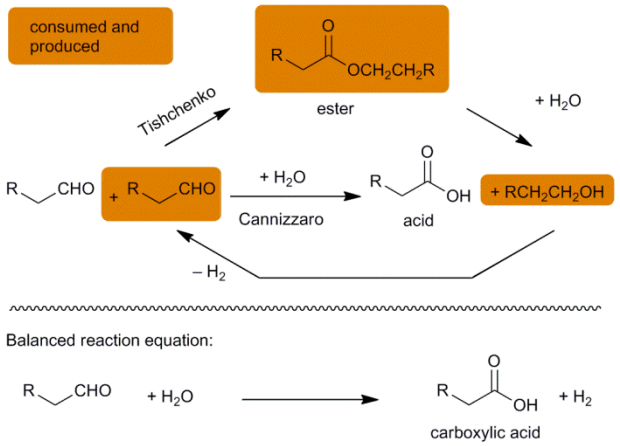

Scheme 6. Oxidation of an aldehyde into a carboxylic acid via the hypothetic reaction pathway involving disproportionation of the aldehyde via Tishchenko or Cannizzaro reaction with subsequent dehydrogenation of the produced alcohol. Two molecules of aldehyde are consumed and one of these recovered so that one molecule of aldehyde is oxidized to one carboxylic acid molecule and one equivalent of hydrogen is produced. Additionally, one water molecule is consumed. The balanced reaction equation coincides with Eq. 3.

Having confirmed by direct detection and a cross-coupling experiment the participation of the corresponding carboxylic acid during the ketonization of an aldehyde, we studied the mechanism of the oxidation at a molecular level.

The formation of a carboxylic acid (derivative) during ketonization by disproportionation, i.e. by Cannizzaro[20, 23, 25, 31] or Tishchenko[17, 18, 21, 45] reaction, has been discussed (Scheme 6) in the literature. There, the alcohol could be dehydrogenated to form one of the two aldehydes and to produce the hydrogen indicated in Eq. 3. Hence, the global reaction equation has exactly the same stoichiometry as Eq. 3 (cf. Scheme 6).

Two reactions were designed to assess whether or not a disproportionation of the aldehyde takes place during its ketonization. First, the ester itself was passed through the catalytic fixed bed reactor and the product mixture was compared to the composition obtained during ketonization of the aldehyde. When starting from the ester, the 7-tridecanone was observed in 31% (Scheme 7) together with carbon dioxide. However, the alcohol (1-heptanol) and 1-heptene were also observed in 13 and 12% yield, respectively (Scheme 7), together with a considerable amount of coke deposited on the catalyst. The fact that 1-heptanol and 1-heptene were not obtained when carrying out the reaction starting from the aldehyde as substrate, excludes the ester as an intermediate in the ketonization of aldehydes. Probably the dehydrogenation of the alcohol to the aldehyde is rather slow, i.e. it is not facilitated effectively by the catalyst and, consequently, this compound accumulates in the reaction media or is consumed in side reactions such as dehydration to give the corresponding olefin. As a consequence, both the alcohol and the olefin are observed.

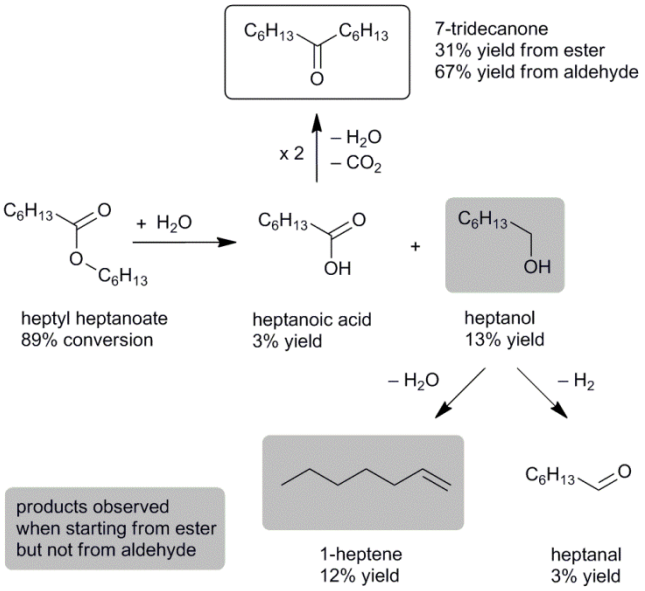

Scheme 7. Product distribution obtained when contacting heptyl heptanoate with *m*-ZrO_2 under reaction conditions of the ketonization of aldehydes. Reaction conditions: heptyl heptanoate (5 mL, 0.2 mL min^{-1}, 2.7 10^4 Pa partial pressure), 50 mL min^{-1} N_2, 1 g catalyst, 450 ºC.

In an additional experiment, we carried out the reaction of the alcohol (1-heptanol) by feeding this separately to the reactor. A product mixture was obtained that contains two main products: the olefin 1-heptene (36%) and the ketonization product 7-tridecanone (23%, Scheme 8) at a conversion of 78%. The aldehyde was only observed in traces. The composition of the mixture confirmed that the alcohol is dehydrated under the reaction conditions to the terminal olefin. As the latter was not observed during the ketonization of aldehydes, the alcohol can also be excluded as reaction intermediate. On the other hand, it can be concluded that the alcohol is dehydrogenated and the aldehyde converted rapidly to the ketonization product. Hence, this demonstrates that the catalyst is active for the dehydrogenation of alcohols.

Scheme 8. Product distribution obtained when contacting heptanol with *m*-ZrO_2 under reaction conditions of the ketonization of heptanal. Reaction conditions: heptanol (5 mL, 0.2 mL min^{-1}, 4.1 10^4 Pa partial pressure), 50 mL min^{-1} N_2, 1 g catalyst, 450 ºC.

As a summary, we can say that the disproportionation of the aldehyde during the ketonization can be excluded. Side products which could indicate the presence of the alcohol during the reaction, e.g. the olefin formed by dehydration or the alcohol itself, were not observed. Therefore, direct dehydrogenation of the aldehyde on the zirconium oxide was considered as a real possibility.

Although zirconium oxide is regarded as a non-reducible catalyst, the hydrogenation of benzoic acid to benzaldehyde has been reported to occur and the coordination of hydride species to the zirconium centers has been proposed by Yokoyama.[19, 46] Interestingly, the hydrogenation of benzoic acid is exactly the reverse reaction of Eq. 3. Hence, from these results it can be concluded that it is not unreasonable to propose the direct dehydrogenation of an aldehyde on a zirconium oxide surface.

With the aim to further explore a possible direct dehydrogenation step, the deuterated aldehyde-*1-d* (see Eq. 6) was employed as substrate. In this case, H–D was expected to be formed as product from the deuterium from the aldehyde and a proton from water or from the surface. Experimentally, the ketonization proceeded smoothly and the ketone product was obtained together with a mixture of H–D and H–H (Eq. 6). The former one was the predicted product whereas the later was rather unexpected. However, Yokoyama et al.[19, 46] indicate that molecular hydrogen (and therewith H–D, once formed and desorbed), can be cleaved heterolytically and adsorbed as proton and hydride species. Furthermore, deuteration of the surface of zirconium oxide by molecular deuterium has been reported by FT-IR.[47] This means that proton/deuterium

exchange with surface hydroxyl groups is possible for molecular deuterium and therewith also proton/deuterium exchange between H–D and water could be expected in the presence of zirconium oxide. This is exactly what was observed when deuterated water was passed together with a hydrogen flow: Hydrogen D–D and H–D were formed (Eq. 7). This result demonstrates unequivocally that surface hydride species are formed under the reaction conditions of the ketonization of aldehydes and this, in turn, explains how a direct dehydrogenation of an aldehyde molecule adsorbed onto a zirconium oxide surface can occur, namely by expulsion of a hydride species which is transferred to the surface. A hydride shift directly from the trigonal planar carbon atom of the aldehyde is unlikely and should rather occur from a tetrahedral carbon atom. In a tetrahedral configuration the aldehyde hydrate can be considered as an analog of a secondary alcohol and the mechanism of the hydride shift analogous to the Meerwein-Ponndorf-Verley reaction. Hence, zirconium oxide has been reported in several cases as an active catalyst for this reaction.[36, 48, 49] The proper configuration can be achieved by reaction of the aldehyde with a surface hydroxyl group. The presence of surface hydroxyl groups has been detected by IR spectroscopy (Figure 4), even after treatment of the oxide at 400 ºC in high vacuum. Probably, these hydroxy groups are related to defect sites on the surface.

From all of the above, the following mechanism for the dehydrogenation of heptanal can be proposed (Scheme 9): The aldehyde is adsorbed onto a surface hydroxyl group by the nucleophilic attack of this group onto the carbon atom forming the required tetrahedral geometry of the carbon atom in the aldehyde. Then, the hydride is transferred to a suitable, Lewis acidic Zr atom. The fusion of two different hydrogen species, i.e. one coordinated to a Lewis acid center and the other to a basic oxygen atom, will release molecular hydrogen. The remaining carboxylate is already prepared to react with a second molecule in the ketonic decarboxylation.

Alternatively, the carboxylic acid can be desorbed and the surface hydroxy group restored. Therefore, a water molecule has to be adsorbed and dissociated, providing the original surface hydroxy group and the proton required for protonation of the carboxylate. It has been proposed before that water can replenish surface oxygen atoms on a cerium oxide surface in the ketonization of aldehydes.[35] A certain hydration and dehydration ability of the ZrO_2 material was detected in the TPD between 200 and 600 ºC (Figure 1). With the displacement of carboxylic acid by a water molecule the catalytic cycle for the aldehyde oxidation by dehydrogenation is closed (Scheme 9) and the reaction equation with all reactants and products involved in the mechanistic cycle has same stoichiometry as Eq. 3 which is in accordance with empirical Eq. 2. Therefore, it can be concluded that this mechanistic cycle is supported by the empirical equation of the long term experiment.

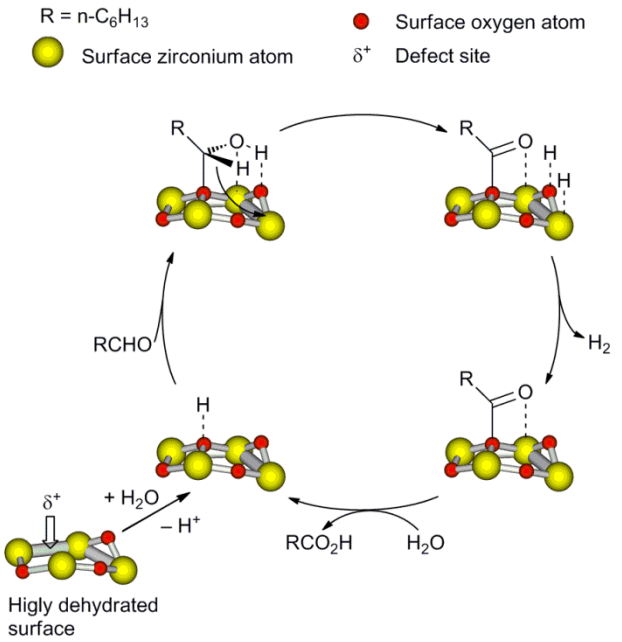

Scheme 9. Proposed mechanism for the dehydrogenation of heptanal (R = C_6H_{13}) to heptanoic acid. A hydride species is transferred from the aldehyde to the surface and molecular hydrogen is formed by recombination of the surface hydride species with a surface proton. Water acts as a hydrogen and oxygen source.

Reaction of water, adsorbed onto the surface and dissociated, with the aldehyde, instead of the surface hydroxyl group, is less likely since in this case addition of water to the feed should accelerate the reaction rate. However, rate retardation was observed instead (Figure 7).

As a summary it can be concluded that experimental results support the ketonization of aldehydes by a dehydrogenation of the aldehyde to the carboxylic acid on a zirconium oxide surface. In this reaction surface hydride species are involved. However, this proposed mechanism should be further confirmed by spectroscopic means, theoretical DFT calculations and kinetic studies.

Kinetic study

It has been shown above that the ketonization of aldehydes consists of two separate reactions: the dehydrogenation of the aldehydes to carboxylic acids and the subsequent ketonic decarboxylation of these acids to the ketone product. When the reaction rate for the formation of the ketone is compared starting from the aldehyde and from the carboxylic acid (Figure S2) it can be seen that ketone formation from the carboxylic acid is straightforward and 2.5 times faster than starting from the aldehyde. From these results it can be concluded that the

carboxylic acid consumption is faster than its formation from the aldehyde. Accordingly, it was observed that the corresponding carboxylic acid was a primary unstable product in the ketonization of aldehydes (Figure 9). Furthermore, in the cross coupling experiment when reacting an aldehyde together with a carboxylic acid (Scheme 5), different product ratios were observed for symmetrical and cross-coupling products, than when reacting two carboxylic acids. This phenomenon is well in line with the explanation that the carboxylic acid possesses a higher reactivity than the aldehyde and the former is rapidly consumed in self-condensation in the presence of an aldehyde and a smaller amount remains available for cross-coupling.

When the slow first reaction step, i.e. the dehydrogenation, was divided into its single steps (Eq. S1 to S3; Supp. Inf.), it can be seen that two of the single steps are quite fast equilibrium processes such as adsorption of the aldehyde, water adsorption and dissociation, or desorption of the reaction product. Even the recombination of the surface hydride species and a surface proton is an equilibrium as it was reported above. Therefore, it can be concluded that the rate-determining step is the hydride transfer from the adsorbed aldehyde to the catalyst surface (Eq. S2, Supp. Inf.) and the rate of the latter depends on the concentration of such surface species. Water has been considered as a competitor for aldehyde adsorption to the active site, i.e. the surface hydroxy group (Scheme 10).

Scheme 10. Proposed competitive adsorption of water to the active *m*-ZrO_2 surface-hydroxy sites.

Then, as the number of surface hydroxy groups is constant on the catalyst (it is assumed that surface hydroxy group resistant to desorption at 450 ºC are related to surface defects), the reaction rate has to be proportional to the concentration of aldehyde in the gas phase. As final rate equation Eq. 8 has been deduced (for more detail see Supp. Inf.; Eq. 8 = Eq. S17):

$$-r_{\mathrm{RCHO}} = \frac{k\,\mathrm{RCHO}}{1 + K_1\,\mathrm{RCHO} + K_4\,\mathrm{H_2O}} \qquad \text{(Eq. 8)}$$

The rate equation was evaluated applying the initial rates method. Initial rates of ketone formation from heptanal were measured at low conversion (< 12%) when the reactant concentration, i.e. its partial pressure in the feed was varied and the water partial pressure was maintained constant at 1.5 10^4 Pa, and depicted in Figure 10. At the same time, the rate equation was also evaluated when the reactant concentration was maintained constant 1.5 10^4 Pa and the water partial pressure was varied in the feed (Figure 7). By means of the SOLVER tool of the EXCEL software a good fitting of Eq. 8 to the experimental data was obtained (cf. Figure 7 and Figure 10). In addition, in a different presentation, i.e. the inverse of the ketone formation rate over the inverse of the aldehyde concentration, a straight line could be drawn fitting all experimental points when varying the aldehyde concentration (Figure S3) or the water concentration (Figure S4). Both graphical solutions support the deduced equation and therewith the hypothesis that the dehydrogenation of the aldehyde coordinated to a surface hydroxy group is the rate determining step.

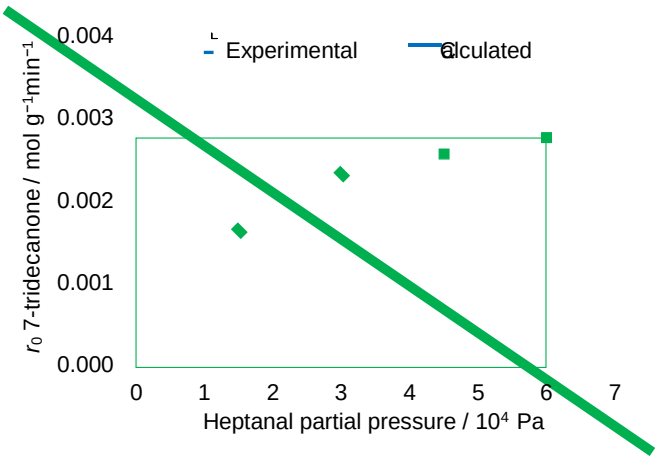

Figure 10. Comparison between experimental and calculated initial reaction rate in heptanal ketonization catalyzed with *m*-ZrO_2 in presence of water (1.5 10^4 Pa) as a function of heptanal partial pressure (1.5, 3, 4.5 and 6 10^4 Pa). The calculated graph was obtained by means of the EXCEL Solver program. Reaction conditions: heptanal (5 mL), water (0.022 mL min^{-1}), heptanal partial pressure 1.5 10^4 Pa (0.636 mL water, 0.169 mL min^{-1} heptanal, 6, 15, 23 mg of catalyst, 136 mL min^{-1} N_2), 3 10^4 Pa (0.319 mL water, 0.350 mL min^{-1} heptanal, 12, 25, 40 mg of catalyst, 110 mL min^{-1} N_2), 4.5 10^4 Pa (0.213 mL water, 0.518 mL min^{-1} heptanal, 15, 25, 40 mg of catalyst, 80 mL min^{-1} N_2) and 6 10^4 Pa (0.159 mL water, 0.69 mL min^{-1} heptanal, 20, 30, 45 mg of catalyst, 50 mL min^{-1} N_2).

The role of the water on the kinetics of the reaction is considered quantitatively only at low conversion in the present paper. As already mentioned before, the role of the water is complex as it influences the overall reaction at least in two or three different ways. Water affects the aldol condensation equilibrium providing additional aldehyde from the aldol condensation product at an advanced stage of the reaction. Furthermore, it has been shown above that the influence of water onto the reaction kinetics of ketonization of carboxylic acids, i.e. on the second reaction of the ketonization of aldehydes, was a clear rate retarding effect (Figure 8). Then, we have also proposed a competitive adsorption to the surface hydroxy groups competing with the aldehyde. So, a rate retarding effect of water on the aldehyde ketonization has been clearly measured (Figure 7) but, probably, there are, at least, three different ways by which the water concentration affects the rate equation, and this issue will not be treated here.

The activation energy was determined in the temperature range of 410 to 450 ºC with *monoclinic* zirconium oxide. The logarithm

of the ketone formation rate is shown in Figure S5 over the inverse reaction temperature. From these data a value of 193 kJ mol^{-1} was calculated for the activation energy. This value is considerably higher than the one for the ketonic decarboxylation of carboxylic acids. For instance, a value of 116 kJ mol^{-1} has been reported for the ketonic decarboxylation of pentanoic acid.[50] Both values are in line with the different reaction controlling step for both reactions as discussed before.

Conclusions

Monoclinic zirconium oxide with a high surface area (> 100 $m^2 g^{-1}$) is an active catalyst for the transformation of aldehydes (heptanal) into symmetrical ketones (7-tridecanone). Although being a non-reducible metal oxide, the material is suitable for this transformation and a yield of 66% has been achieved.

The reaction mass balance shows that water is consumed and hydrogen is formed. Moreover, carbon dioxide is formed during the transformation of the aldehyde into the ketone. In this reaction no sacrificial oxidant was necessary since water plays this role by providing hydrogen and oxygen atoms at the same time.

Water has a beneficial effect on product selectivity when using *monoclinic* zirconium oxide as catalyst. This has been explained by a shift in the composition for aldol condensation equilibrium. Thus, the aldol condensation by-product is minimized and the liberated aldehyde can react towards the desired product.

Concerning the reaction mechanism, the carboxylic acid has been identified as reaction intermediate and it is proposed that in a key-step, the aldehyde is adsorbed onto the metal oxide surface and a hydride species is transferred to the surface. These findings are interesting and may help to improve the catalyst for instance by incorporating metal sites which can facilitate this hydride transfer.

Experimental Section

General

Heptanal was purchased from Aldrich and distilled under reduced pressure before used. Water was employed in deionized form. *Monoclinic* zirconium oxide (*m*-ZrO_2) and *tetragonal* zirconium oxide (*t*-ZrO_2) were purchased from ChemPur, Germany, as pellets and *monoclinic* zirconium oxide (*m*-ZrO_2-A) was obtained from Aldrich as a powder. Cerium oxide (nanopowder) was received from Rhodia. Heptanoic acid, heptanal and *p*-toluenesulfonic acid monohydrate were supplied by Sigma-Aldrich.

Catalyst characterization

The X-ray diffraction measurements of *m*-ZrO_2, *t*-ZrO_2, *m*-ZrO_2-A, and CeO_2 were carried out to confirm crystallinity of the active phases. Analyses were performed on a PANalytical CUBIX-PRO diffractometer equipped with a PW3050 goniometer (Cu Kα radiation) provided with a variable divergence slit. Nitrogen physisorption isotherms were obtained using a Micromeritics ASAP 2420 analyzer. Catalysts were out-gassed in vacuum at 200 ºC prior to the analysis until the static pressure remained less than 70 Pa. The Brunauer–Emmett–Teller (BET) method was used to calculate the surface area in the range of relative pressures between 1 and 20 Pa. Temperature programmed reduction (TPR) for CeO_2, *m*-ZrO_2, *t*-ZrO_2 and *m*-ZrO_2-A catalysts was carried out on a conventional flow apparatus (Autochem 2910, Micromeritics). A 0.3-g sample was pretreated in an O_2 (2%)/He flow at 550 ºC for 1 h and cooled in a He flow to room temperature, followed by Ar purge. The sample was then reduced in a H_2 (10%)/Ar flow. Temperature was increased from room temperature to 950 ºC at a constant heating rate of 10 K/min and held for 5 min. Water produced during the reduction was eliminated with a frozen *n*-propanol trap and the amount of consumed H_2 was monitored by a thermal conductivity detector (TCD).

The Lewis acidity of CeO_2, *m*-ZrO_2, *t*-ZrO_2 and *m*-ZrO_2-A catalysts was characterized by NH_3-temperature programmed desorption (NH_3-TPD). The analysis was carried out using an Autochem II, chemisorption analyzer. A sample (0.1 g) was pretreated in an O_2 flow at 450 ºC for 30 min. The sample was cooled down to 176 ºC in an argon flow and saturated with NH_3 in He at a flow rate of 10 mL min^{-1}. Desorption was carried out by heating the sample at 10 K/min from 176 to 600 ºC. The TPD profile of the catalysts was recorded using a TCD detector and the compounds desorbed were identified with a mass spectrometer OmniStar, Balzers instrument. The infrared measurements on the catalysts were performed with a Nicolet iS10 spectrometer using a vacuum cell. The solids were employed as self supported wafers of 1 cm diameter and 15–25 mg weight, which were degassed for 1 h under vacuum (0.1 to 1 Pa) at room temperature. IR spectra were recorded at room temperature, also after a treatment at 300 and 400 ºC in vacuum.

Catalytic tests in a fixed-bed, continuous-flow reactor

Transformations of heptanal and alternative reactions (hexanal-aldol condensation product, hexanal-heptanal mixture, heptanal-heptanoic acid mixture, heptanoic-hexanoic acid mixture, heptyl heptanoate and heptanol) were carried out in a tubular stainless-steel reactor. The catalyst (1.0 g, pellets 0.4 – 0.8 mm) was diluted with silicon carbide (2.0 g), placed as a fixed bed in a stainless-steel tube (0.4 cm internal diameter and 20 cm length) and calcined at 450 ºC for 2 h in air (50 mL min^{-1}). The reactor was heated to different reaction temperatures between 300 to 450 ºC. Heptanal (0.2 mL min^{-1}) and water were fed separately into the reactor with molar ratio of 1 : 8 together with a nitrogen flow of 50 mL min^{-1} at ambient pressure. Heptanal, the reaction mixtures and the substrates mentioned before (5 mL aliquots) were passed through the reactor at 450 ºC, with a rate of 0.2, 0.167 or 0.140 mL min^{-1} together with a gas flow of 50, 185 or 213 mL min^{-1} at ambient pressure, as stated in the corresponding figures. The liquid product was condensed with an ice bath and analyzed offline by GC with an Agilent 7890A apparatus, equipped with a HP-5 column (30 m, 0.32 mm, 0.25 µm) and a FID detector, using *n*-dodecane (Aldrich) as an external standard. Gaseous products were trapped in a gas burette and analyzed by GC on a Varian 450 with a “refinery gas analyzer” configuration with three channels. Hydrogen was analyzed after separation on a 2 m molecular sieve 5 Å column by a thermal conductivity detector. Permanent gases such as CO and CO_2 were separated on a 2.5 m molecular sieve 13X column and quantified by a thermal conductivity detector. Low molecular weight hydrocarbons were separated on a 50 m Plot/Al_2O_3 column and quantified with a flame ionization detector. 7-Tridecanone was distilled from the reaction mixture and identified by mass spectroscopy and ^{13}C NMR and ^{1}H NMR spectroscopy (see Supp. Inf.). For testing the catalyst stability, 15 portions of heptanal (7.33 g) and water (9.2 g), molar ratio 1 : 8, were fed consecutively into the reactor (1.0 g *m*-ZrO_2) at 450 ºC without intermediate catalyst calcinations. Liquid and gas phases were analyzed by GC as mentioned above.

Isotopically labeled experiments in a fixed-bed, continuous-flow reactor

Transformation of heptanal-*1-d* was done as described above at 450 ºC over 1.0 g (pellets 0.4 – 0.8 mm) of *m*-ZrO_2. Heptanal-*1-d* (2 mL, 0.09 mL min^{-1}) and water (1.275 mL, 0.057 mL min^{-1}) were fed separately into the reactor with a molar ratio of 1: 5 with a nitrogen flow of 10 mL min^{-1} at ambient pressure. The liquid product was condensed with an ice bath and analyzed offline by GC. Gaseous products were trapped in a gas burette and analyzed by GC and MS on a Mass Spectrometer-OminStar/ThermoStar (Software Quadera QMG220 version 4.40). Heptanal-*1-d* conversion was 89% and the corresponding ketone, 7-tridecanone, was achieved in 61% yield. The experimental molar yields of hydrogen deuteride (HD) and hydrogen (H_2) were 46% and 26% respectively. In comparison, the experimental global amount of H_2 obtained for the non-deuterated heptanal was 58%.

In order to prove hydrogen-deuterium exchange over *m*-ZrO_2, an amount of H_2 (14 mL min^{-1}) similar to the one produced during the reaction was fed in presence of D_2O (1.4 mL, 0.057 mL min^{-1}) and N_2 (10 mL min^{-1}). For H_2, DH and D_2, yields of 14%, 25% and 19% were obtained, respectively. When the same experiment was carried out over SiC (silicon carbide) H/D exchange was not observed.

Kinetic measurements of initial rates in a fixed-bed, continuous-flow reactor.

Kinetic measurements were carried out in a tubular stainless-steel reactor at 450 ºC and ambient pressure using 0.2 – 0.4 mm pellets of *m*-ZrO_2. Adequate N_2 and heptanal flow rates were selected to avoid heat and mass transfer limitations. With the aim to determine the kinetic expression of the reaction, initial rates of formation of the principal product (7-tridecanone) were calculated by keeping heptanal partial pressure and total flow constant while the contact time (W/F) was varied by employing different amounts of catalyst. Heptanal conversions were not higher than 12 %.

Initial rates were calculated for different partial pressures feeding 5 mL of heptanal with partial pressures of 1.5, 3, 4.5 and 6 10^4 Pa, using heptanal flow of 0.169, 0.350, 0.518 and 0.690 mL min^{-1} respectively. In this series, nitrogen flow was kept constant (144 mL min^{-1}).

To test the initial rate effect of adding water to the reaction, heptanal partial pressure of 1.5 10^4 Pa was maintained constant using heptanal flow of 0.147 mL min^{-1}, while heptanal : water molar ratio was varied from 1: 1 to 1: 3 and 1: 5. Kinetic modeling to fit the experimental data with the proposed rate expression was carried out using the Excel Solver program. The activation energy for the heptanal reaction was determined in the temperature range of 410 to 450 ºC using heptanal flow of 0.147, N_2 flow of 144 mL min^{-1} and 23 mg of *m*-ZrO_2.

Acknowledgements

The authors thank MINECO (CTQ2011-27550, Consolider Ingenio 2010-MULTICAT and Severo Ochoa program, SEV-2012-0267) and Generalitat Valenciana (PROMETEO II/2013/011 Project) for funding this work. L.M.O. is grateful to the COLCIENCIAS institute for a Francisco-Jose-de-Caldas (512/2010) doctoral fellowship.

Keywords: biomass conversion • carboxylic acid • heterogeneous catalysis • hydride shift • kinetic study

[1] M. J. Climent, A. Corma, S. Iborra, *Green Chem.* **2014**, *16*, 516-547.
[2] D. Y. Murzin, I. L. Simakova, *Catal. Ind.* **2011**, *3*, 218-249.
[3] J. N. Chheda, G. W. Huber, J. A. Dumesic, *Angew. Chem. Int. Ed.* **2007**, *46*, 7164-7183.
[4] G. W. Huber, S. Iborra, A. Corma, *Chem. Rev.* **2006**, *106*, 4044-4098.
[5] A. Pulido, B. Oliver-Tomas, M. Renz, M. Boronat, A. Corma, *ChemSusChem* **2013**, *6*, 141-151.
[6] G. W. Huber, J. N. Chheda, C. J. Barrett, J. A. Dumesic, *Science* **2005**, *308*, 1446-1450.
[7] J. Q. Bond, D. M. Alonso, D. Wang, R. M. West, J. A. Dumesic, *Science* **2010**, *327*, 1110-1114.
[8] A. Corma, O. de la Torre, M. Renz, N. Villandier, *Angew. Chem. Int. Ed.* **2011**, *50*, 2375-2378.
[9] A. Corma, O. de la Torre, M. Renz, *Energ. Environ. Sci.* **2012**, *5*, 6328-6344.
[10] B. G. Harvey, H. A. Meylemans, *Green Chem.* **2014**, *16*, 770-776.
[11] R.-J. van Putten, J. C. van der Waal, E. de Jong, C. B. Rasrendra, H. J. Heeres, J. G. de Vries, *Chem. Rev.* **2013**, *113*, 1499-1597.
[12] E. F. Iliopoulou, *Curr. Org. Synth.* **2010**, *7*, 587-598.
[13] M. Gliński, G. Zalewski, E. Burno, A. Jerzak, *Appl. Catal. A: Gen.* **2014**, *470*, 278-284.
[14] T. N. Pham, T. Sooknoi, S. P. Crossley, D. E. Resasco, *ACS Catal.* **2013**, *3*, 2456-2473.
[15] M. Renz, *Eur. J. Org. Chem.* **2005**, 979-988.
[16] R. S. Murthy, P. Patnaik, P. Sidheswaran, M. Jayamani, *J. Catal.* **1988**, *109*, 298-302.
[17] F. Hayashi, M. Tanaka, D. Lin, M. Iwamoto, *J. Catal.* **2014**, *316*, 112-120.
[18] H. Idriss, E. G. Seebauer, *J. Mol. Catal. A: Chem.* **2000**, *152*, 201-212.
[19] T. Yokoyama, N. Fujita, T. Maki, *Appl. Catal. A: Gen.* **1995**, *125*, 159-167.
[20] S. M. Kim, M. E. Lee, J.-W. Choi, D. J. Suh, Y.-W. Suh, *Catal. Commun.* **2011**, *16*, 108-113.
[21] Y. Kamimura, S. Sato, R. Takahashi, T. Sodesawa, T. Akashi, *Appl. Catal. A: Gen.* **2003**, *252*, 399-410.
[22] S. Sato, R. Takahashi, T. Sodesawa, K. Matsumoto, Y. Kamimura, *J. Catal.* **1999**, *184*, 180-188.
[23] V. I. Komarewsky, J. R. Coley, *Adv. Catal.* **1956**, *8*, 207-217.
[24] J. B. Claridge, M. L. H. Green, S. C. Tsang, A. P. E. York, *J. Chem. Soc., Faraday Trans.* **1993**, *89*, 1089-1094.
[25] S. Ananthan, N. Venkatasubramanian, C. N. Pillai, *J. Catal.* **1984**, *89*, 489-497.
[26] Y. Wang, B. H. Davis, *Appl. Catal. A: Gen.* **1999**, *180*, 277-285.
[27] J. Wrzyszcz, H. Grabowska, R. Klimkiewicz, L. Syper, *Appl. Catal. A: Gen.* **1999**, *185*, 153-156.
[28] H. Teterycz, R. Klimkiewicz, B. W. Licznerski, *Appl. Catal. A: Gen.* **2001**, *214*, 243-249.
[29] J. Bussi, S. Parodi, B. Irigaray, R. Kieffer, *Appl. Catal. A: Gen.* **1998**, *172*, 117-129.
[30] S. Foraita, J. L. Fulton, Z. A. Chase, A. Vjunov, P. Xu, E. Baráth, D. M. Camaioni, C. Zhao, J. A. Lercher, *Chem. Eur. J.* **2015**, *21*, 2423-2434.
[31] A. Gangadharan, M. Shen, T. Sooknoi, D. E. Resasco, R. G. Mallinson, *Appl. Catal. A: Gen.* **2010**, *385*, 80-91.
[32] M. Kobune, S. Sato, R. Takahashi, *J. Mol. Catal. A: Chem.* **2008**, *279*, 10-19.
[33] N. Plint, D. Ghavalas, T. Vally, V. D. Sokolovski, N. J. Coville, *Catal. Today* **1999**, *49*, 71-77.
[34] J. Wrzyszcz, H. Grabowska, R. Klimkiewicz, L. Syper, *Catal. Lett.* **1998**, *54*, 55-58.
[35] T. S. Hendren, K. M. Dooley, *Catal. Today* **2003**, *85*, 333-351.
[36] K. Tanabe, T. Yamaguchi, *Catal. Today* **1994**, *20*, 185-197.

[37] S. Wan, T. Pham, S. Zhang, L. Lobban, D. Resasco, R. Mallinson, *AIChE J.* **2013**, *59*, 2275-2285.
[38] A. Corma, L. M. Orozco, M. Renz, *New Journal of Chemistry* **2013**, *37*, 3496-3502.
[39] J.-R. Kim, W.-J. Myeong, S.-K. Ihm, *Appl. Catal. B Environ.* **2007**, *71*, 57-63.
[40] T. J. Farmer, M. Mascal, in *Introduction to Chemicals from Biomass*, John Wiley & Sons, Ltd, **2015**, pp. 89-155.
[41] H.-B. Hu, K.-W. Park, Y.-M. Kim, J.-S. Hong, W.-H. Kim, B.-K. Hur, J.-W. Yang, *J. Ind. Eng. Chem. (Seoul)* **2000**, *6*, 238-241.
[42] H. Idriss, C. Diagne, J. P. Hindermann, A. Kiennemann, M. A. Barteau, *J. Catal.* **1995**, *155*, 219-237.
[43] M. V. Ganduglia-Pirovano, A. Hofmann, J. Sauer, *Surf. Sci. Rep.* **2007**, *62*, 219-270.
[44] G. da Silva, J. W. Bozzelli, *J. Phys. Chem. A* **2006**, *110*, 13058-13067.
[45] S. Y. Onozawa, T. Sakakura, M. Tanaka, M. Shiro, *Tetrahedron* **1996**, *52*, 4291-4302.
[46] T. Yokoyama, T. Setoyama, N. Fujita, M. Nakajima, T. Maki, K. Fujii, *Appl. Catal. A: Gen.* **1992**, *88*, 149-161.
[47] T. Merle-Mejean, P. Barberis, S. Ben Othmane, F. Nardou, P. E. Quintard, *J. Eur. Ceram. Soc.* **1998**, *18*, 1579-1586.
[48] C. Battilocchio, J. M. Hawkins, S. V. Ley, *Org. Lett.* **2013**, *15*, 2278-2281.
[49] T. Komanoya, K. Nakajima, M. Kitano, M. Hara, *J. Phys. Chem. C* **2015**, *119*, 26540-26546.
[50] B. Oliver-Tomás, F. Gonell, A. Pulido, M. Renz, M. Boronat, *Catal. Sci. Technol.* **2016**, in press; DOI: 10.1039/C1036CY00395H.

Entry for the Table of Contents (Please choose one layout)

Layout 1:

FULL PAPER

Text for Table of Contents

((Insert TOC Graphic here: max. width: 5.5 cm; max. height: 5.0 cm))

*Author(s), Corresponding Author(s)**

Page No. – Page No.

Title

Layout 2:

FULL PAPER

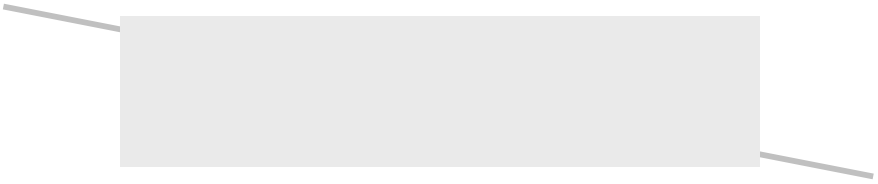

L. M. Orozco, M. Renz and A. Corma**

Page No. – Page No.

Carbon-carbon bond formation and hydrogen production in the ketonization of aldehydes

By isolating molecular hydrogen as a co-product in the ketonization of aldehydes its sacrificial oxidation to water is avoided and the energy liberated in the oxidation of an aldehyde into a carboxylic acid can be recovered stored in this molecule. The hydrogen source is water. It is confirmed that the carboxylic acid is the intermediate in the ketonization of aldehydes and the second step is the classical decarboxylation of carboxylic acids.